Solubility of Ni, Cu and Minor Elements in FeO_X-SiO_2-MgO Slag Equilibrating with Nickel Alloy

Romeo U. Pagador
Mitsuhisa Hino
Kimio Itagaki

Institute For Advanced Materials Processing (IAMP)
Tohoku University
2-1-1 Katahira, Aoba-Ku
Sendai 980-77, Japan
Tel. no. 81-22-217-5151
Fax no. 81-22-217-5211

ABSTRACT

In order to obtain the fundamental data in ferro-nickel and cupro-nickel smelting, equilibrium experiments between magnesia saturated FeO_X-SiO_2-MgO slags and liquid Cu-Ni-Fe alloys were carried out under controlled oxygen potential at 1673 and 1773K. The MgO solubility in the FeO_X-SiO_2 slag increases from 16 to 32 mass% with increasing SiO_2 content at 1773K. The Ni and Cu contents in the slag decrease with reducing oxygen potential or increasing temperature. By comparing the values of the distribution ratio, $L_x^{s/m}$, Fe will remain basically in the slag while Ni and Cu will concentrate in the alloy phase. At 1673K, the Ni dissolution will be lower than Cu at P_{O2} = $3x10^{-4}$ Pa. Based on the logarithmic relationship between the distribution ratio and the oxygen potential, the predominant species dissolved in the slag are NiO, $CuO_{0.5}$, FeO, CoO and $SbO_{1.5}$. Using the activity values of Ni and Cu determined by a Knudsen cell mass spectrometer, the activity coefficients of NiO and $CuO_{0.5}$ in the slag were estimated to be approximately 3.5 and 4 to 7, respectively. The high content of MgO does not significantly affect the dissolution of these metals in slag.

1. INTRODUCTION

With the limited natural resources and the rapid depletion of higher grade sulfidic ores, greater attention is now focused on the treatment of other resources. Laterite ores, although containing lower grades, represent more than 3/4 of the world's estimated reserves for nickel[1]. These large and relatively underdeveloped resources have the potential of becoming an increasingly important source for nickel. Lateritic ores particularly garnierite which is the main raw material for Fe-Ni production contains very high levels of silica and magnesia. Thus this work is undertaken to provide basic information on metal losses during laterite smelting. Nickel solubility in silicate slags had been investigated by several researchers [2-5]. However, there are no reported papers on slags with high magnesia content or on the effect of magnesia on the solubility of metals in slag equilibrating with nickel alloys. Furthermore, the basic data on nickel alloys and slag equilibria related to ferro-nickel and cupro-nickel production process are limited. Equilibrium experiments between magnesia saturated FeO_X-SiO_2-MgO slag and liquid Cu-Ni-Fe alloy were carried out to determine the solubility of Ni, Cu and few minor elements in slag. The activity coefficients of the component elements in the slag phase were also estimated to analyze their behavior in the smelting process.

2. EXPERIMENTAL PROCEDURE

Three grams of high purity Ni alloyed with three grams of copper were equilibrated with five grams of pre-melted fayalite slag in a dense sintered magnesia crucible at 1673 and 1773K. In some experiments antimony and sulfur were added in the form of Ni_5Sb_2 and Ni_3S_2 master alloys while metallic cobalt was directly charged with the sample. To prevent the premature erosion of the magnesia crucible, some amount of magnesia powder was also added in the charge. The CO and CO_2 gas mixture was used to maintain the oxygen potential from 10^{-1} - 10^{-5} Pa over the slag melt. The gas train was connected with a moisture absorber and a capillary flowmeter with a bleeder system to regulate the gas flow. The stream of purified and dried CO/CO_2 gas passing over the sample was approximately 100 ml/min at the standard state.

The schematic diagram of the furnace assembly is shown in Fig. 1. A silicon carbide heating element was used to heat up the furnace. The temperature was controlled by a SCR controller which maintained the temperature to within ±2K and measured by an alumina shielded Pt-Pt13%Rh thermocouple lodged on the refractory platform beside the holding crucible. The CO/CO_2 gas mixture enters the reaction chamber through an alumina tube that was inserted into the holding crucible. Both ends of the reaction chamber were sealed by silicon rubber stoppers to prevent the ingress of air.

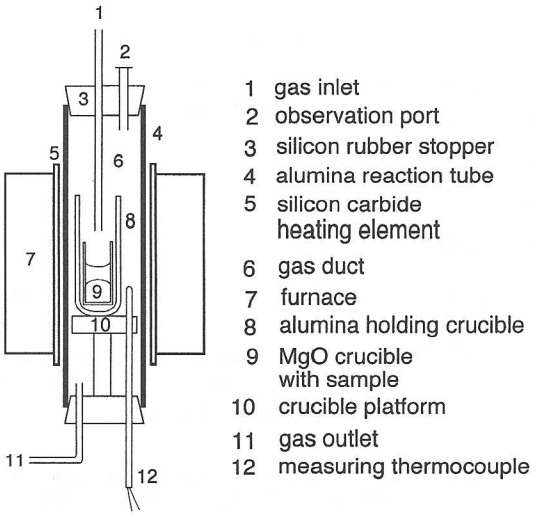

Fig. 1. Schematic diagram of the reaction tube assembly.

The experimental system has seven components (Ni, Cu, Fe, Si, Mg, O and C) and four phases (alloy, slag, gas and crucible). Based on the phase rule, the degree of freedom is five. These can be accommodated by specifying the temperature, total pressure of the system, Ni/Cu ratio, CO/CO_2 ratio and the Fe content in the alloy or the SiO_2 content in the slag in the present investigations.

In a typical run, the metal alloy and the slag were loaded inside a 50 mmH x 11 mmID magnesia crucible. This was placed in a 100 mmH x 17 mmID alumina holding crucible and then hooked with a molybdenum wire. The sample was gradually lowered to the constant temperature zone after the desired CO/CO_2 gas ratio has been set. After attaining the equilibrium time, the sample was quickly taken out of the furnace and quenched in nitrogen atmosphere. Ni, Cu and other elements were analyzed by using the ICP while silica was determined gravimetrically. The Fe^{2+} content in the slag was analyzed by titration with $K_2Cr_2O_7$ after dissolving the sample in a stream of CO_2 gas.

3. EQUILIBRIUM TIME

A series of experiments were carried out to determine the time required to reach equilibrium. Initially, the Ni-Cu alloy was melted with the slag and held at 1673K for 12 to 60 hours. The oxygen partial pressure was maintained at $2x10^{-4}$ Pa. The results are shown in Fig. 2 where the mass% Ni in slag is plotted against holding time. The equilibrium condition was also approached from the slag side with the addition of 3 mass% NiO under the same condition. After 40 hours, the Ni content in the slag from both sides has approached the level of 0.65 mass%. The Cu content in the slag was different but a similar trend was observed in the Cu solubility with holding time. The study showed that it takes 40 hours for the equilibrium between the metal and the slag phase to be established. Subsequently, all samples were maintained at the set temperature under a constant gas flowrate of CO/CO_2 for 44 hours before quenching.

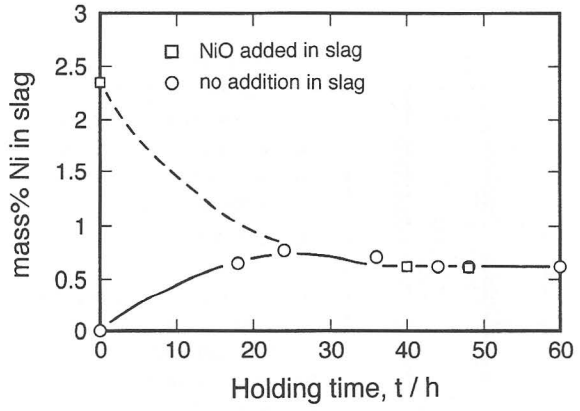

Fig. 2. Change of nickel content in slag with the holding time at $\log p_{O2} = -8.6$ at 1673K.

4. EXPERIMENTRAL RESULTS

4.1 MgO Solubility in Slag

The MgO solubility in the FeO_X-SiO_2 slag is shown in Fig 3. The MgO solubility increases with increasing silica content. At 1673K, the MgO content in slag is around 8 mass% corresponding to around 10 mass% SiO_2. This increases to around 17 mass% when the SiO_2 content is increased to 30 mass%. The MgO solubility increases about 5 mass% on the average when the temperature was increased by 100K.

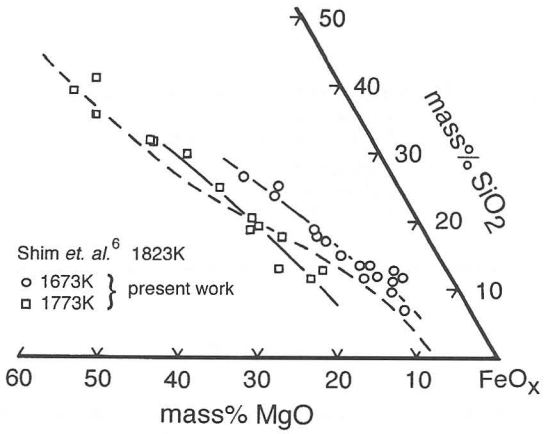

Fig. 3. MgO solubility in the FeO_X-SiO_2 fayalite slag equilibrating with the Ni-Cu-Fe alloy at 1673 and 1773K.

Since the FeO_X-SiO_2-MgO slag is basically used in the converting process of the iron smelting where the operating temperatures are much higher than this experimental condition, the MgO solubility curve at temperatures below 1823K is not available. The MgO solubility in FeO_X-SiO_2 slag equilibrating with liquid iron under inert gas atmosphere at 1873K was reported by Shim *et al.* and their results are plotted in broken lines in Fig. 3 [6]. While the alloy phases in both experiments are different, similar MgO solubilities are observed at the lower FeO content region. This could be attributed to the significantly high Fe content in the Cu-Ni alloy at the reduced oxygen potential. However, the MgO solubility near the FeO_X corner is much higher because, in this region of higher oxygen potential, the high dissolution of Ni and Cu in the slag increases the MgO solubility to be larger than that reported by Shim.

4.2 Fe^{3+}/Fe^{2+} Ratio in Slag

The $(Fe^{3+}/Fe^{2)}$ ratio is one factor of knowing the degree of oxidation of Fe in the slag. The FeO and $FeO_{1.5}$ relationship is given by reaction 1

$$FeO(l) + 1/4\ O_2(g) = FeO_{1.5}(l) \qquad (1)$$

and from the equilibrium relationship,

$$\log(Fe^{3+}/Fe^{2+}) = \log K_1 + 1/4 \log p_{O2} + \log(\gamma_{FeO}/\gamma_{FeO1.5}) \qquad (2)$$

where K_1 is the equilibrium constant of reaction 1. From Eq. (2), if the ratio of the activity coefficients is constant, the log(Fe^{3+}/Fe^{2}) and the oxygen potential will give a linear relationship with a slope equal to 1/4. Fig. 4 shows the relationship between log(Fe^{3+}/Fe^{2}) and the oxygen potential at 1673 and 1773K. With increasing oxygen potential, the FeO in slag is oxidized and the $FeO_{1.5}$ content increases. At $\log p_{O2}$ = -6, the (Fe^{3+}/Fe^{2}) ratio is about 0.5 and about 1/3 of the total Fe in slag is of the form $FeO_{1.5}$. At $\log p_{O2}$ = -9, the Fe^{3+} content in slag is decreased to less than 10%. The figure also shows that at the same oxygen potential, when the temperature is increased, the (Fe^{3+}/Fe^{2}) ratio is decreased. The linear relationship between log(Fe^{3+}/Fe^{2}) and the oxygen potential has a slope of near 1/4 thus the ($\gamma_{FeO}/\gamma_{FeO1.5}$) ratio in Eq. (2) is almost constant.

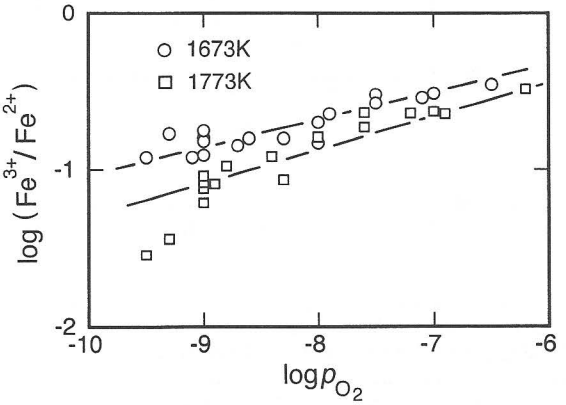

Fig. 4. Relationship between (Fe^{3+}/Fe^{2+}) ratio and the oxygen potential at 1673 and 1773K.

4.3 Nickel and Cu Solubility in Slag

The nickel content in slag equilibrating with an alloy where the ratio of (mass% Ni/mass% Cu) is equal to 1 is plotted against the oxygen potential in Fig. 5. The general trends show that the solubility of Ni in slag increases with increasing oxygen potential. At 1673K, the Ni in slag increases from 0.4 to over 8 mass% when the oxygen potential is increased from $\log p_{O2}$ = -9 to - 6.5. Increasing the temperature decreases the Ni solubility in slag at constant oxygen potential.

In this series of experiments, the composition of the alloy phase can be changed even for the same oxygen potential as explained in the degree of freedom. By varying the Ni content of the alloy, the consequent change in the mass% Ni in slag was found to be very small. For example, the Ni content in slag increased slightly from 0.08 to 0.14 mass% when the Ni content in the alloy was increased from 19 to 34 mass% at constant $\log p_{O2}$ = -9 at 1773K. In the nickel matte smelting process, the nickel activity in matte is similar with that in the present alloy[7]. If 0.5 mass% Ni is accepted as the nickel dissolution in slag, then the process can be operated at $P_{O2} = 10^{-4}$ Pa at 1673K based on the present result. In order to reduce Ni loss in slag further would require a further reduction of the oxygen potential.

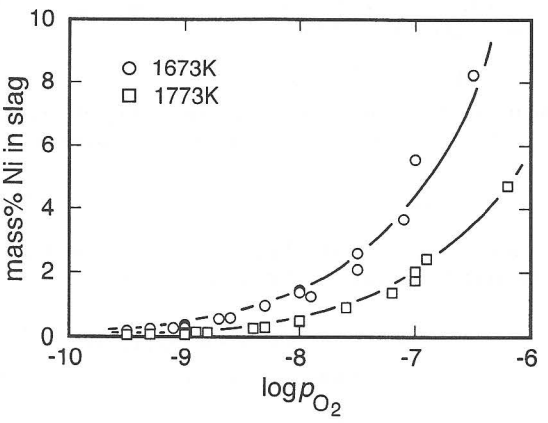

Fig. 5. Relationship between the Ni solubility in slag and $\log p_{O2}$ at 1673 and 1773K.

Similar trends can be observed for the Cu solubility in slag as shown in Fig. 6. The mass% Cu in slag decreases with decreasing oxygen potential and increasing temperature. The experiment similar to the Ni solubility was carried out for the Cu dissolution in slag at $\log p_{O2}$ = -9 at 1673 and 1773K. In the case of copper, there is a bigger change in the copper solubility with changes in the copper content in the alloy. This difference in the copper and nickel solubility with varying alloy contents will be discussed in the distribution ratio. By comparing Fig 5 and 6, the Cu content in slag is lower than Ni at high oxygen potential but becomes higher than the Ni solubility at the lower oxygen potential region.

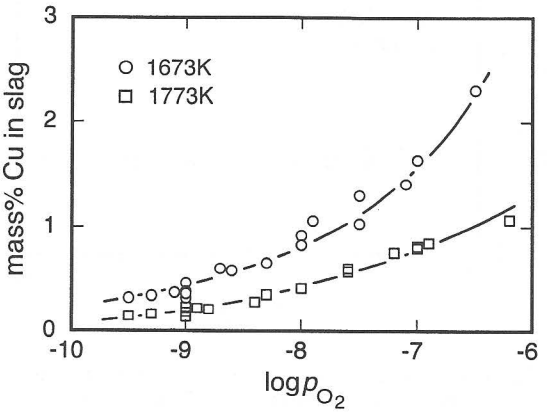

Fig. 6. Relationship between the Cu solubility in slag and $\log p_{O2}$ at 1673 and 1773K.

5. DISCUSSION

5.1 Oxidic Dissolution of Metal in Slag

The distribution ratio of an element X between the slag and metal phases in this investigation is defined as

$$L_X^{s/m} = (\text{mass\% X in slag})/[\text{mass\% X in alloy}] \quad (3)$$

This relationship can be reasonably explained based on the metal-metal oxide equilibria where

$$X(l) + \nu/4O_2(g) = XO_{\nu/2} \quad (4)$$

and the valence of the metal X is ν and $XO_{\nu/2}$ is represented with one cation base. The equilibrium constant K_4 for reaction 4 is given by

$$K_4 = a_{XO\nu/2}/a_X \cdot p_{O2}{}^{\nu/4} \quad (5)$$

By rearranging Eq. 5, the distribution ratio of an element X between metal and slag is given by Eq (6)

$$\log L_X^{s/m} = \log\{(n_T)/[n_T]\} + \log\{[\gamma_X]/(\gamma_{XO\nu/2})\} + \log K_4 + \nu/4 \log p_{O2} \quad (6)$$

where ( ) and [ ] denote the values in the slag and the alloy phases respectively and n_T is the total number of moles in 100g of each phase. If the ratios of the activity coefficients and the total number of moles in the slag and alloy phases are kept constant, the linear relationship between the logarithmic plot of the $L_X^{s/m}$ and the oxygen partial pressure would suggest the valence of the dissolved species in slag.

Fig. 7 shows the relationship between the $(n_T)/[n_T]$ and the oxygen potential. The total number of moles per 100g sample is around 1.6 - 1.7 in both slag and metal phases. While the oxygen potential changed over the experimental range, the $(n_T)/[n_T]$ ratio almost remained constant. This experimentally determined factor in Eq. 6. does not significantly affect the relationship between the distribution ratio and the oxygen potential.

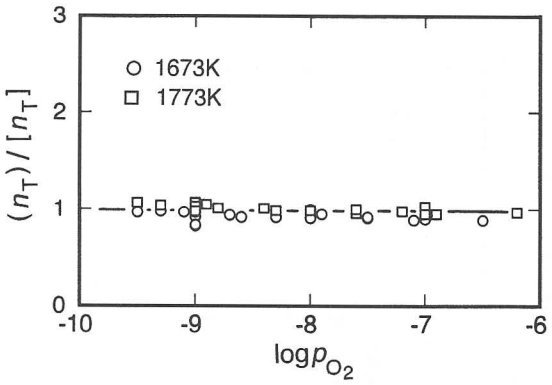

Fig. 7. Relationship between the $(n_T)/[n_T]$ ratio and the oxygen potential at 1673 and 1773K.

5.2 Distribution Ratio

The distribution ratios of Ni, Cu and Fe are plotted against the oxygen potential in Fig. 8. To make a clearer figure, the distribution ratio of Fe is given at 1673 and 1773K while those for Ni and Cu are at 1673K. The experimental data for Ni and Cu at 1773K will be presented later. Looking at the general trends, the distribution ratios increase with increasing oxygen potential. Also the distribution ratio for Fe shifted downwards with increase in temperature. From the slope of the distribution ratio against the oxygen potential, the valence of the metal dissolved in slag can be estimated by applying Eq. (6).

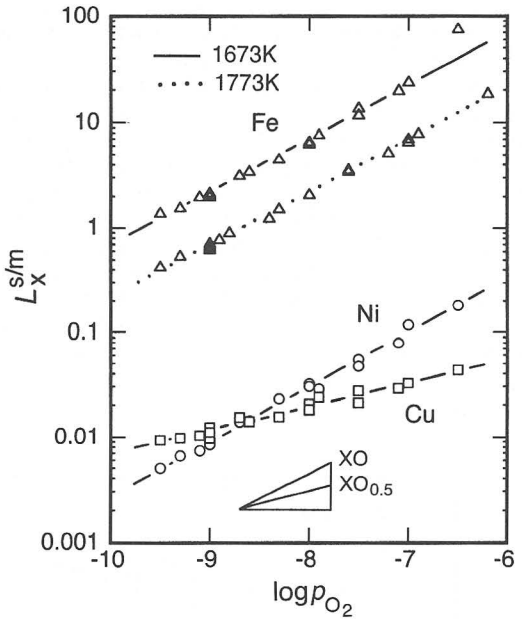

Fig. 8. Relationship between $L_X^{s/m}$ and $\log p_{O2}$ for Fe at 1673 and 1773K and Ni and Cu at 1673K.

Judging from the value of the distribution ratio, $L_{Fe}^{s/m}$ is greater than 1 indicating that Fe will distribute mainly in the slag phase. On the other hand, the values for Ni and Cu are very low and are expected to make up the alloy phase. At 1673K and $\log p_{O2}$ = -9, the $L_{Ni}^{s/m}$ is about 1/100. However when the oxygen potential is increased to -7, the distribution ratio becomes 10 times more.

The distribution ratio lines for Ni and Cu cross at about $\log p_{O2}$ = -8.6 at 1673K. In the oxygen partial pressure range below this value, the Cu dissolution in the slag is higher than Ni. Thus in highly reductive smelting such as the Fe-Ni operation, the Cu dissolved in the slag is expected to be higher than Ni. On the other hand, at the higher oxygen potential representative of the Ni and Cu smelting, the Cu and Ni loss in the slag should be a major concern.

In this research regarding Ni and Cu alloy (where the Ni/Cu ratio is equal to 1) and slag equilibrium, varying the oxygen potential can be done but keeping the alloy composition constant is difficult to maintain. This is because the distribution ratio of Fe changes with changes in the oxygen potential and accordingly, the alloy composition also changes even if the charge composition is kept constant. From Fig. 8, at $\log p_{O2}$ = -9 the $L_{Fe}^{s/m}$ is 2. Keeping the mass% Fe in slag to less than 30% is difficult because silica saturation occurs at about 40% FeO_X. Thus the Fe content in the slag can be varied only from 16-35 mass%. At $\log p_{O2}$ = -7, the $L_{Fe}^{s/m}$ is 30. Since the maximum content of FeO_X in the present study is about 90% FeO_X, the mass% Fe in the alloy cannot be higher than 2.5%. Thus in carrying out these experiments over a wide oxygen potential region, the alloy composition consequently must change in a wide range.

To know the behavior of Fe, the slag composition was varied from 50 - 87 and 29 - 52 mass% Fe at $\log p_{O2}$ = -9, for 1673 and 1773K respectively. The change in the distribution ratio of Fe is small and almost constant. This suggests that even with changes in the slag composition, the $L_{Fe}^{s/m}$ is almost fixed and basically is only a function of the oxygen potential.

5.3 Distribution Ratio of Ni

The distribution ratio of Ni obtained in the present study is exhibited in Fig 9. From the figure, the distribution ratio decreases with decreasing oxygen potential. Also with increasing temperature, the distribution ratio decreases for the same oxygen potential. As was previously discussed, the alloy composition can be varied even with a fixed oxygen potential. From the figure, the distribution ratios changed very slightly while the Ni content in the alloy was varied from 33 - 39 and 19 - 34 mass% for 1673 and 1773K respectively at $\log p_{O_2}$ = -9. The $L_{Ni}^{s/m}$ is also basically a function of the oxygen partial pressure.

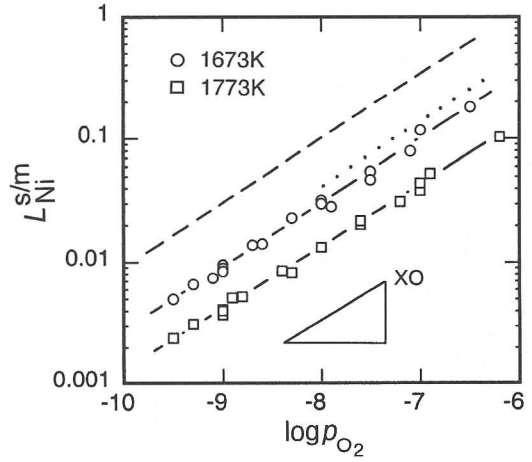

Fig. 9. Relationship between $L_{Ni}^{s/m}$ and $\log p_{O2}$ at 1637 and 1773K.
---- Wang *et al.* at 1573K [2,3]
..... Taylor *et al.* at 1673K [4]

There are very few investigations on the equilibrium between nickel alloy and fayalite silicate slag while the Ni and Cu solubility in MgO saturated FeO_X-SiO_2-MgO slag had not been reported. Wang *et al.* investigated the Ni solubility in Ni-Cu and Ni-Au alloy equilibrating with silica saturated slag[2,3]. The distribution ratio calculated from their data at 1573K is plotted in broken lines in Fig 9. If the temperature dependence is considered, the present results are consistent with their data. Similarly, Taylor and Jeffes reported the slag composition and rounded figures of the alloy composition in the investigation on the equilibrium between the Ni-Cu alloy and silica unsaturated silicate slag at 1673K[4]. Their results that are plotted in the dotted lines in Fig. 9 agree with the present result. Because of the similar tendencies of the distribution ratio $L_{Ni}^{s/m}$ in the present study when compared to the silicate slags, the MgO content in slag does not show a significant effect on the dissolution of Ni in the slag. From these investigations as well as the present data, the linear relationship between $\log L_{Ni}^{s/m}$ and the oxygen potential shows a slope of 1/2. This suggests that the predominant species of Ni in slag is NiO.

5.4 Distribution Ratio of Copper

The relationship between the distribution ratio of Cu and the oxygen potential is plotted in Fig. 10 . The general tendencies are similar with Ni. The distribution ratio increases with oxygen potential and decreasing temperature. The dependence of $L_{Cu}^{s/m}$ with the oxygen potential is more scattered when compared with $L_{Ni}^{s/m}$. While there are many investigations on the Cu metal and slag equilibrium related to the copper smelting process, there are very limited reports on the dissolution of Cu equilibrating with Ni/Cu alloy. Wang *et. al.* investigated the Cu solubility in silica saturated slag equilibrating with Ni/Cu alloy at 1573K as shown in broken lines in the figure[2]. The present results agree with their report if the temperature dependence is considered in this study. Takeda *et al.* also reported the Cu solubility in the FeO_X-SiO_2 slag using an MgO crucible at 1673K as shown by the dotted lines in Fig.10 [8]. Deviation of their results could be attributed to the different composition of the Cu-Ni-Fe alloy and the corresponding $[\gamma_{Cu}]$ in their study as expressed in Eq. 6. Similarly comparing the $L_{Cu}^{s/m}$ with their slag system, the MgO content in slag again shows no significant effect on the dissolution of Cu. From the figure, the linear relationship between the $L_{Cu}^{s/m}$ and the oxygen potential is near 1/4 thus the species of Cu dissolved in slag is of the form $CuO_{0.5}$.

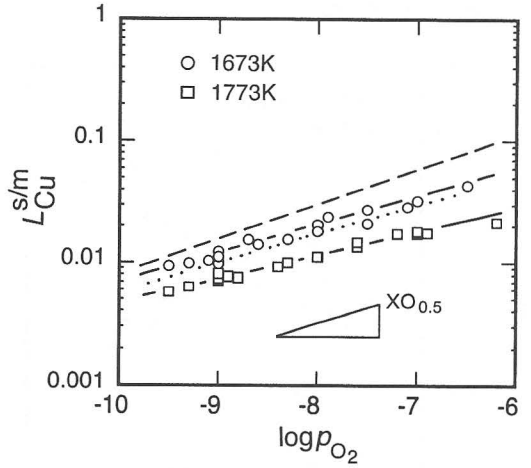

Fig. 10. Relationship between $L_{Cu}^{s/m}$ and $\log p_{O2}$ at 1673 and 1773K.
---- Wang *et al* at 1573K [2]
..... Takeda *et al.* at 1573K [8]

5.5 Distribution Ratios of Minor Elements

To determine the solubility of minor elements in the slag, cobalt, antimony and sulfur were added as a metal or a master alloy separately with the charge. The amount of each element was limited to less than 5 % of the total alloy weight. Fig. 11 shows the relationship of the distribution ratios of Co, Sb and S against the oxygen potential at 1673 and 1773K. Looking at the tendency of $L_{Co}^{s/m}$, cobalt is distributed in the slag phase but then concentrates in the alloy phase at the lower oxygen potential. The value of $L_{Co}^{s/m}$ decreases by 0.1 when the oxygen potential is increased from 10^{-2} to 10^{-4} Pa at 1673K. The linear relationship between $\log L_{Co}^{s/m}$ and $\log p_{O2}$ has a gradient of about 1/2. This suggests that the predominant species of cobalt in the slag phase is CoO. Comparing Figs. 9 and 11,

the distribution ratio of cobalt is higher than nickel. Thus, cobalt will dissolve more in slag than nickel. At the lower oxygen potential region, the dissolution of cobalt in slag may even be lower than Cu because of the difference in their slopes. The antimony solubility in the slag is very low. At these experimental temperatures, the antimony content in the slag is hardly detected particularly at the lower oxygen potential. From the figure, the distribution ratio of antimony is very low and as such would distribute itself mainly in the alloy phase. Judging from the value of $L_{Sb}^{s/m}$, it will be very difficult to remove antimony even at the higher oxygen potential. Over the experimental region, the dissolved species of antimony is presumed to be $SbO_{1.5}$. However, the slope of the relationship between $\log L_{Sb}^{s/m}$ and $\log p_{O_2}$ is nearer to 1/2 and does not agree with the expected slope. The distribution ratio is affected greatly by the activity coefficients of both the alloy and the slag phases as expressed by Eq. 6. The Fe content in the alloy phase increases with decreasing oxygen potential. The activity coefficient of antimony is not available at dilute solution in the Cu-Ni-Fe alloy. However, γ_{Sb} in the Ni-Cu alloy must increase by the addition of Fe because the γ_{Sb} in Fe-Sb system shows a larger value compared to the Cu-Sb and Ni-Sb systems[9,10]. The distribution ratio of S against the oxygen potential shows a reverse trend. Keeping the mass% S in the alloy to around 4, the mass% S in slag increase with decreasing oxygen potential. Thus the distribution ratio of sulfur decreases with increasing oxygen potential as seen in Fig.11.

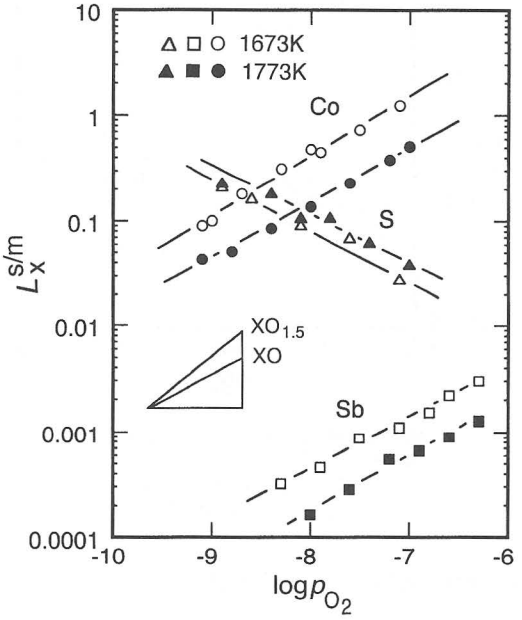

Fig. 11. Relationship between $L_x^{s/m}$ and $\log p_{O_2}$ at 1673 and 1773K.

5.6 Activity Coefficients in the Metal Phase

The activity coefficient of minor elements in slag is required to analyze the behavior of these elements in the smelting process. For this purpose, the activity coefficient of the elements in the slag phase is estimated in the present study. The activity coefficients of Ni, Cu and Fe in the ternary alloy had been determined by mass spectrometric measurements at 1623K[11]. The activity coefficient of Ni in the alloy composition range where the ratio of mass% Ni/ mass% Cu is equal to 1 is almost constant as listed in Table I. This is expected from the Cu-Ni binary system where the activities of Ni and Cu show almost ideal behavior[12]. The addition of Fe in the Ni-Cu alloy phase does not cause a significant change in the activity coefficient of nickel. The activity coefficient of Ni in the ternary alloy was estimated to be about 1.4 after extrapolating the $[\gamma_{Ni}]$ at the experimental temperature by assuming that the regular solution model holds. Inputting this value in Eq.6 would give the (γ_{NiO}) equal to 3.5.

Table I. Calculated activity coefficients of Ni and Cu in the Cu-Ni-Fe ternary system at 1623K.

	$L_x^{s/m}$	$[\gamma_X]$	$(\gamma_{XO_{v/2}})$
Ni	0.181 - 0.0055	1.3 -1.4	3 - 3.5
Cu	0.043 - 0.0087	1.3 -2.3	4 - 7

On the other hand, the behavior of Cu in the alloy phase is different from Ni. The iso-activity curves of copper in the Cu-Ni-Fe ternary alloy at 1623K is illustrated in Fig. 12. As can be seen in the figure, the $[\gamma_{Cu}]$ increases with increasing Fe content in the alloy. This can be expected from the behavior of Cu in the binary system. The Ni-Cu binary represents almost ideal behavior but the Cu-Fe binary shows very positive deviation from ideality[13]. The addition of Fe in the Cu-Ni binary must show a positive change in the activity coefficient of copper as shown in Table I. Increasing Fe content in the alloy phase with decreasing oxygen potential causes a tendency of the $L_{Cu}^{s/m}$ to increase according to Eq. (6). This behavior of Cu in the alloy phase could explain the scattering of points and the linear dependency of less than 1/4 in Fig 10. Comparing the $L_{Cu}^{s/m}$ of alloys with almost the same Fe content in the alloy would show a linear tendency of about 1/4. Similarly plugging the $[\gamma_{Cu}]$ corresponding to the alloy composition into Eq. (6) would give the value of 4 to 7 for $(\gamma_{CuO_{0.5}})$.

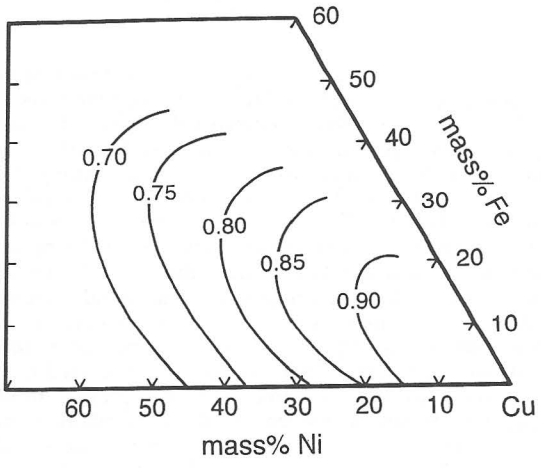

Fig. 12. Iso-activity curves of Cu in the Cu-Ni-Fe ternary system at 1623K.

6. CONCLUSION

The phase relations between MgO saturated FeO_X-SiO_2-MgO slag and nickel alloys were undertaken to obtain basic information related to the ferro-nickel and cupro-nickel smelting. The results of this investigation are as follows:

1. The MgO solubility in the FeO_X-SiO_2 slag increased from 8 to 17 mass% corresponding to 10 to 30 mass% SiO_2 at 1673K. The MgO solubility curve shifts by about 5 mass% when the temperature was increased from 1673 to 1773K.

2. The Ni and Cu solubility in slag increases with increasing oxygen potential at constant temperature. Increasing the temperature decreases the dissolution of Ni and Cu in slag .

3. Basing on the value of $L_x^{s/m}$, Fe will remain mostly in the slag phase while Ni and Cu will be concentrated in the alloy phase. At 1673K, the Cu content in the slag will be higher than Ni at $\log p_{O_2}$ lower than 3×10^{-4} Pa because of the difference in the slopes of $L_x^{s/m}$ against $\log p_{O_2}$.

4. From slope of the linear relationship between the distribution ratio and the oxygen potential, the species dissolved in the slag are estimated to be of the forms NiO, $CuO_{0.5}$ and CoO and $SbO_{1.5}$ is expected for antimony.

5. Using the activity values of Ni and Cu derived from the mass spectrometric measurement of the alloy phase, the activity coefficients of NiO and $CuO_{0.5}$ were estimated to be 3.5 and 4 to 7 respectively.

6. The MgO content has minor effect on the dissolution of these metals into the slag phase.

REFERENCES

1. B. Terry, "Pyrometallurgy of Sulfide ores of Nickel to Finished Metal or Mattes," Extractive Metallurgy of Nickel, John Wiley & Sons, New York, 1987, pp. 8-50.

2. S.S. Wang, A.K. Kurtis and J.M. Toguri, "Distribution of Copper-Nickel and Copper-Cobalt between Copper-Nickel and Copper-Cobalt Alloys and Silica Saturated Fayalite Slag," Can. Metall. Quart., Vol. 4, 1973, pp. 383-390.

3. S.S. Wang, N.H. Santander and J.M. Toguri, "The Solubility of Nickel and Cobalt in Iron Silicate Slags," Metall. Trans., Vol. 5, 1974, pp. 261-265.

4. J.R. Taylor and J.H Jeffes, "Slag-Metal Equilibria between Nickel-Copper Alloys and Iron Silicate Slags of Varying Composition," Trans. IMM, Vol. 21C, 1974, pp. C136-C148.

5. M. Nagamori, "Metal Loss to Slag: Part II. Oxidic Dissolution of Nickel in Fayalite Slag and Thermodynamics of Continuous Converting of Nickel-Copper Matte," Metall. Trans., Vol. 5, 1974, pp. 539-548.

6. J. D. Shim and S. Banya, "The Solubility of Magnesia and Ferric-Ferrous Equilibrium in Liquid FeO_T-SiO_2-CaO-MgO Slag," Tetsu to Hagane, Vol. 67, 1981, pp. 79-88.

7. J.M. Larrain and S.L. Lee, "Thermodynamic Properties of Copper-Nickel and Sulfur Melts," Can. Metall. Quart., Vol. 19, 1980, pp. 183-190.

8. Y. Takeda, S. Kanesaka and A. Yazawa. "Equilibria between FeO_X-CaO-SiO_2 Slag and Liquid Cu-Ni-Fe Alloy," Proceedings for Nickel Metallurgy, edited by E. Ozberk and S.W. Marcuson, Vol. 1. CIM 1986, pp. 185-202.

9. M. Hino, J.I. Kim and T. Azakami, "Antimony Activities in Sb-X (X: Fe, Co, Ni) Binary Alloys," Bulletin of the Institute for Advanced Materials Processing, Vol. 50 No. 1,2, Dec. 1994, pp. 38-46.

10. S. Itoh and T. Azakami, "Activity Measurements of Bismuth and Antimony in Liquid Copper Base Binary Alloys by Knudsen Effusion Method with Electrobalance," J. of Jpn. Inst. Met., Vol. 48, no 4, 1984, pp 405-413.

11. Y. Fujita, "Activity Measurements in Nickel Base Alloys by Mass Spectrometer," Masters Thesis, Tohoku University ,1996

12 A.D. Kulkarni and R.E. Johnson, "Thermodynamic Studies in Liquid Copper Alloys by Electromotive Force Method: Part II. The Cu-Ni-O and Cu-Ni Systems," Metall. Trans., Vol. 4, 1973, pp. 1723-1727.

13. U.V. Choudary, J.A. Serkin and G.R. Belton, "A Mass-Spectrometric Study of the Thermodynamics of the Fe-Cu and Fe-Cu-C_{sat} Systems at 1600 °C," Metall. Trans., Vol. 6B, 1975, pp. 399-403.